

Origin of the vibrational shift of CO chemisorbed on Pt(111)

F. Illas, S. Zurita, and J. Rubio

Departament de Química Física, Facultat de Química, Universitat de Barcelona, C/Martí i Franqués 1, 08028 Barcelona, Spain

A. M. Márquez

Departamento de Química Física, Facultad de Química, Universidad de Sevilla, 41012 Sevilla, Spain

(Received 21 February 1995; revised manuscript received 6 June 1995)

Ab initio self-consistent field and complete active space self-consistent field cluster-model wave functions have been obtained for a CO-Pt₄ cluster model simulating the atop interaction of CO on Pt(111). The origin of the vibrational shift between free and chemisorbed CO has been investigated by means of the constrained space orbital variation method. This analysis shows that the vibrational shift is the result of several effects. First, there is a large positive shift due to Pauli repulsion, and second various negative contributions; these are substrate polarization, σ donation, and π back donation, respectively. This theoretical analysis shows that the mechanism suggested by Blyholder is, in fact, the one responsible for the observed vibrational shift.

I. INTRODUCTION

Due to its direct relationship to industrial catalytic processes involving CO reactions on Pt-based catalysts, chemisorption of CO on Pt(111) has been one of the most extensively studied systems in surface science. Now, it is well established that CO chemisorbs nondissociatively on Pt(111) leading to regular structures where the metal surface is almost perfect.¹ A variety of experimental techniques show that, at low coverages, CO is chemisorbed mainly at atop sites with the molecular axis perpendicular to the surface and in a C-down orientation.²⁻⁹ When the coverage is increased, two different species are observed. These species have been assigned as chemisorbed CO above the atop and bridge sites of the Pt(111) surface. This assignment has been confirmed through quantitative analysis of the low-energy electron diffraction (LEED) pattern of the $c(4 \times 2)$ phase.¹

Electronic energy-loss spectroscopy vibrational measurements for the CO/Pt(111) system at very low exposure show two peaks at 465 and 2100 cm⁻¹, which are assigned to the C-Pt and C-O stretching modes. When the CO exposure is increased, two new bands at 350 and 1870 cm⁻¹ appear. These two new bands are assigned to the corresponding C-Pt and C-O vibrational modes of bridge chemisorbed CO.^{4,5} This is in agreement with the quantitative LEED analyses mentioned above.¹ A common feature of the two vibrational bands assigned to the C-O stretching mode is that they are shifted with respect to the internal normal mode of free CO, which is 2170 cm⁻¹.¹⁰ In fact, the appearance of these vibrational shifts is precisely used as a guide to determine adsorption sites.¹¹ Thus, it is customary to assign the peaks in the

≈ 2130 – 2000 -cm⁻¹ region to atop sites, the ≈ 2000 – 1800 -cm⁻¹ region to bridge sites, and the ones appearing at ≈ 1880 – 1650 cm⁻¹ to hollow sites.^{11,12} Here we must point out that, although this approach has been widely used to assign adsorption sites, its applicability has been questioned recently.^{13,14}

The first attempt to explain the origin of the CO stretching mode vibrational shift in terms of a mechanism of CO bonding to metal surfaces was given as early as 1964 by Blyholder.¹⁵ According to this mechanism, also known as σ donation– π back donation mechanism, bonding occurs because of a charge transfer from the 5σ orbital of CO to the unoccupied metal orbitals followed by a charge transfer, or back donation, from the d_{π} metal orbitals to the $2\pi^*$ unoccupied level of CO. The validity of the Blyholder mechanism has been theoretically proven in a wide number of different systems. This includes metal-carbonyl complexes, small metal-CO molecules, and CO on metal surfaces.¹⁶⁻²² An often ignored important point is that for late transition metals such as Cu, or for d^{10} metal-carbonyl complexes, the only important mechanism is precisely the back donation.²¹⁻²³ A detailed analysis of the different contributions to the vibrational shift for CO on Cu(100) and Pd(100) has been reported by Bagus and co-workers.²⁴⁻²⁶ These authors have used a new theoretical method of analysis, the constrained space orbital variation method,²⁷⁻²⁹ to show that there are two main physical contributions to the vibrational shift of chemisorbed CO. The constrained space orbital variation (CSOV) method allowed Bagus and co-workers to show that there is a large positive shift due to the Pauli repulsion between the frozen electronic densities of the chemisorbed molecule and that of the sur-

face known as a "wall effect." This effect is almost canceled by a large negative shift due to the donation from metal d_π to the CO $2\pi^*$ orbitals; this is precisely the back donation mechanism.

In spite of the large body of theoretical evidence in favor of the validity of the donation-back donation mechanism in carbonyl complexes or in CO above surface cluster models, some authors have claimed that the frequency and intensity of the CO stretching modes in metal carbonyl can be explained without recourse to this bonding mechanism.^{30,31} We must point out that these works were published well before the theoretical analyses of Bagus and co-workers and, hence, were not aware of the theoretical proof of the Blyholder mechanism, at least for the case of CO on Cu(100). However, in a recent theoretical cluster model study Ohnishi and Watari³² argue that the Blyholder mechanism does not hold for CO on Pt(111). These authors report a vibrational frequency of 1830 cm^{-1} for CO interaction with an atop Pt atom of a cluster model simulating the Pt(111). The vibrational shift with respect to the calculated free CO is not reported, but their value represents a shift of -340 cm^{-1} with respect to the experimental vibrational frequency of free CO. According to the usual assignments, this vibrational frequency is too low for CO interacting at the atop site. Regardless of this large vibrational shift Ohnishi and Watari state that because the CO $2\pi^*$ level lies above the Fermi level, the back donation mechanism cannot contribute to the CO-Pt bonding.³² A similar conclusion is reached from theoretical model studies by Volphilhac, Baba, and Achard³³ where the CO-Pt interaction is found to be weak and involving only the 5σ orbital of CO.

In this work, we will report an *ab initio* cluster-model study of the interaction of CO at the atop site of a Pt(111) surface model. We will be especially concerned with the origin of the vibrational shift of the CO internal stretching mode. An analysis of the results using the CSOV method allows us to identify the leading mechanisms of these vibrational shifts. We will unambiguously show that the mechanisms for this vibrational shift are consistent with the Blyholder model and, also, with previous studies for CO interacting with other metal surfaces.

II. SURFACE CLUSTER MODEL AND COMPUTATIONAL DETAILS

In this work we use a Pt_4 cluster model to simulate the atop interaction of CO with the onefold atop site of the Pt(111) surface. Our model contains only one surface atom and three atoms in the second layer with the geometry fixed at the bulk value (Fig. 1). The symmetry point group of the surface cluster model is C_{3v} . Because of the limitations of such a surface model it is not possible to obtain accurate results for some properties as the interaction energy. However, local properties such as equilibrium geometries or vibrational frequencies are usually well reproduced by small cluster models. More important than obtaining accurate values for these quantities is the proper understanding of the adsorbate-surface chemical bond. Here, the cluster-model approach is especially well suited considering that high-quality *ab ini-*

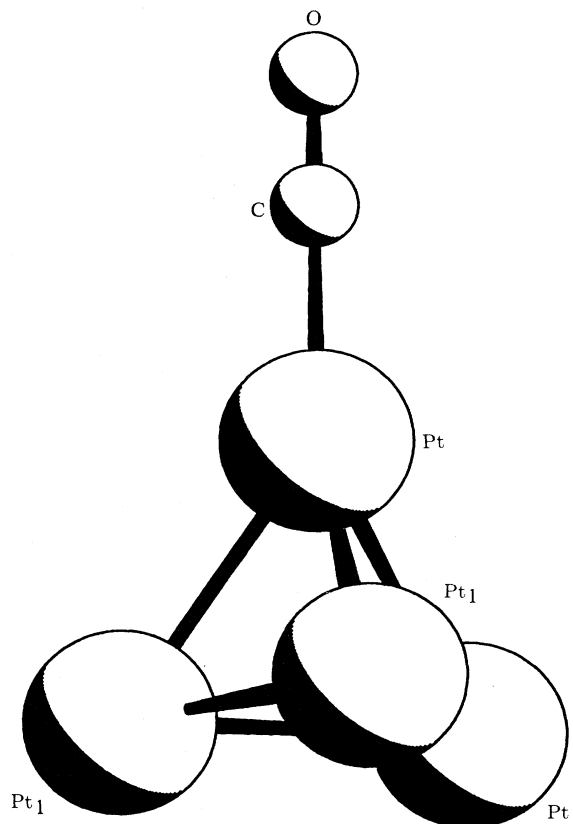


FIG. 1. Schematic representation of the CO-Pt₄ cluster model of CO above the atop site of the Pt(111) surface.

tio wave functions can be obtained and analyzed (see Ref. 34, and references therein).

Ab initio calculations for transition-metal clusters, even for a small Pt_4 model, may be rather involved. This is not only due to computational requirements, which today should not be a problem, but because of the existence of d open shells, which lead to a very large number of electronic states in a small energy range ($\approx 0.2\text{ eV}$). A way to solve the problem is the use of pseudopotentials to describe the inner cores of the Pt atoms. However, if the $5d^96s^1$ electrons of each Pt atom are explicitly included we will still have the same problem with the number of low-lying electronic states. Therefore, we have decided to include the $5d^96s^1$ electron of the atop Pt atom only. The rest of Pt cluster atoms are treated as one-electron pseudoatoms and the inner cores (including an averaged d^9 shell) are represented by a recently developed one-electron pseudopotential. The use of this mixed pseudopotential approach permits us to take into account the interaction of the CO orbitals with the $5d$ orbitals of the atop Pt atom, which are rather local, and enables a modest description of the s or conduction band.

The ten-electron pseudopotential for the atop Pt atom has been constructed following the nonempirical formalism of Durand and co-workers.³⁵⁻³⁷ The different s , p , d , and f potentials have been obtained from an all-electron relativistic self-consistent field (SCF) calculation carried out in a very large basis set of Slater-type orbitals for the

Pt atom. The s potential has been constructed to match the relativistic all-electron $6s$ orbital of the Pt atom in the $5d^9 6s^1(^3D)$ configuration. The p potential is obtained in a similar way but from an atomic calculation in the $5d^9 6p^1(^3F)$. For the d potential we have followed a different approach and used a mixture of the potentials extracted from relativistic SCF calculations in the $5d^9 6s^1(^3D)$ and the $5d^{10}(^1S)$ electronic state. The mixture between these two d potentials has been carried out to reproduce at best the Hartree-Fock limit energy differences corresponding to the $5d^9 6s^1(^3D)$, $5d^8 6s^2(^3F)$, and $5d^{10}(^1S)$ multiplets. This procedure is similar to that suggested by Fernández Pacios³⁸ but here the different weight given to each potential is optimized. Finally, the f potential has been obtained from a calculation for the f^1 configuration of Pt^{9+} . This procedure enables one to obtain an f potential acting in the region of the $5d$ atomic orbitals.³⁹ The one-electron pseudopotential is constructed in a similar manner but contains a spherically averaged d hole. This pseudopotential has been previously used in a study of Pt_3 and Pt_4 bare clusters⁴⁰ and of the PtH and PtH^+ diatomic molecules.⁴¹

For the ten-electron atop Pt atom we use a Gaussian-type orbital (GTO) basis set containing $6s$, $4p$, and $6d$ primitive GTO's contracted to $3s$, $2p$, and $3d$; this is abbreviated as $(6s4p6d/3s2p3d)$. For the one-electron Pt pseudoatoms we use a $(5s3p/2s1p)$ basis set. For CO we use the triple zeta plus polarization contraction of the Dunning $(10s, 6p, 1d)$ primitive set.⁴² Here we must point out that results obtained with the above described basis set are almost unchanged when larger basis sets, $(7s7p6d2f/5s5p4d2f)$ and $(6s3p/4s2p)$, are employed to describe the cluster Pt atoms.⁴³

Using the above-mentioned pseudopotentials and basis sets we have obtained *ab initio* Hartree-Fock, SCF, and multiconfigurational Hartree-Fock self-consistent field wave functions for the Pt_4 -CO supersystem. For the multiconfigurational case the complete active space self-consistent field (CASSCF) method was used.

We have considered always a C-down interaction and a vertical orientation; the symmetry point group of the supersystem is again C_{3v} . In order to understand the non-dynamical correlation contribution to the vibrational frequency of free and chemisorbed CO, several CASSCF wave functions were used. In each case, we have optimized both C-Pt and C-O internuclear distances and calculated the vibrational frequencies corresponding to the normal mode perpendicular to the surface, the frustrated translation, and the internal CO stretching. The high- and low-frequency separation method⁴⁴ has been used to obtain the two vibrational frequencies at the equilibrium geometries. The calculated values for these two different vibrational modes differ by one order of magnitude, thus justifying the present uncoupled approach. The vibrational frequencies have been obtained from a cubic analysis of a polynomial fit to seven points around the minimum of the corresponding energy curve. In order to identify the origin of the C-O vibrational shift we have carried out an analysis of the vibrational frequency using CSOV method.²⁷⁻²⁹

All calculations have been carried out on a locally

modified version of HONDO8.5 package^{45,46} running on IBM RISC-6000 workstation.

III. RESULTS AND DISCUSSION

The electronic structure of the Pt_4 bare cluster itself is a complicated matter because of the various possible spin and space coupling between the atop Pt atom d -hole and the electronic structure arising from the $6s$ "conduction-band" electrons. In the C_{3v} point group the four conduction-band electrons lead to an $a_1^2 e^2$ electronic configuration with the open-shell electrons coupled to a 3A_2 term. The atop Pt d orbitals are split into $e + e + a_1$ symmetry species due to the symmetry lowering from spheric symmetry to the C_{3v} point group. Therefore, the d^9 electronic configuration becomes either $e^4 e^4 a_1^1(^2A_1)$ or $e^4 e^3 a_1^2(^2E)$ and coupling with the s -band electrons leads to $a_1^2 e^4 e^4 a_1^2 e^1(^2E)$, $a_1^2 e^4 e^4 a_1 e^2(^4A_2)$, or $a_1^2 e^4 e^3 a_1^2 e^2(^4E)$. Upon interaction with CO the relevant low-lying electronic states are the same provided CO is a closed-shell molecule. At the SCF levels these electronic states are separated by ≈ 0.15 eV for Pt_4 and by ≈ 0.40 eV for Pt_4 -CO. For the Pt_4 -CO system the lowest electronic state is 2E with an e^1 open shell and is the one chosen in this work to represent the atop interaction of CO with $Pt(111)$. A detailed description of the results concerning the remaining electronic states for both Pt_4 and Pt_4 -CO will be reported elsewhere.⁴³

The C-Pt and C-O distances and the two vibrational modes, frustrated translation and internal CO stretching, for the 2E electronic ground state have been obtained at the SCF and CASSCF levels, where we have indeed considered several active spaces. In the CASSCF method, the wave function is univocally determined once the number of active electron and active orbitals is specified. For Pt_4 -CO the first CAS, hereafter referred to as CAS1, contains 9 electrons in 8 active orbitals. The active orbitals are all of e symmetry and correspond (approximately) to the d_π orbitals of the Pt atop atom, the 1π and $2\pi^*$ of CO, and the e open shell. The second CAS, CA2, involves 9 electrons in 10 orbitals. It is the same as CAS1 but adds another virtual orbital of d_π character with an extra node. Finally, we have considered a third CAS, CAS3, which involved 7 electrons in 8 orbitals. In this case, we consider as active orbitals those dominated by the 5σ , 1π , $6\sigma^*$, and $2\pi^*$ orbitals of CO plus the e open shell mainly of cluster s -band character. A more detailed description of each of the above described active spaces is schematically given in Fig. 2. In all CASSCF calculations the contribution of the SCF configuration to the final CASSCF wave function is always larger than 94%. This is a clear indication of the adequacy of the SCF approach to describe the CO- Pt_4 interaction.

Results for the Pt-C and C-O distances and for the vibrational frequency corresponding to the frustrated translation are reported in Table I. The SCF and different CASSCF values for the C-Pt distance are very close and are of the order of the experimental value. In fact, the calculated values are of ≈ 2.0 Å to be compared with 1.85 ± 0.1 Å as reported by Ogletree, Van Hove, and Somorjai.¹ The SCF and CASSCF calculated C-O dis-

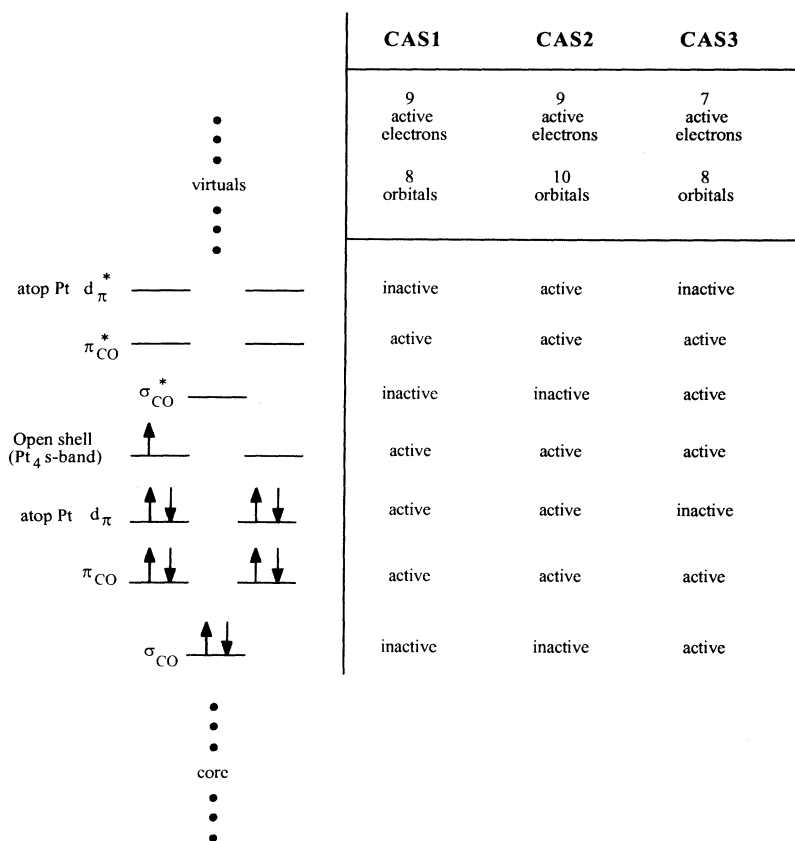


FIG. 2. Schematic representation of the electronic structure of the Pt₄-CO system showing the dominant character of each orbital. The different complete active spaces used in the CASSCF calculations are also indicated.

tances are also close to the experimental value. For the SCF we have obtained an optimum distance of 1.10 Å whereas the different CASSCF calculations lead to values of 1.12–1.13 Å and the experimental value is 1.15±0.05 Å.¹ Similar results were obtained in the local density functional (LDF) study of Ohnishi and Watari who report a C-Pt distance of 2.09 Å and a C-O distance of 1.13 Å.³² Hence, both the SCF (or CASSCF) and the LDF approach lead to equilibrium geometries that are close to the experimental values. Interestingly enough the cluster equilibrium geometries are close to those reported for the simple Pt-CO system by either Smith and Carter (1.99 and 1.13 Å, using generalized valence bond and dissociation consistent configuration interaction methods⁴⁷) or Roszak and Balasubramanian (1.90 and 1.15 Å, from relativistic CASSCF followed by multireference configuration interaction calculations⁴⁸).

The vibrational frequency for the frustrated translation calculated at SCF or CASSCF levels is very similar but is quite different from that corresponding to the Pt-CO system. In fact, the present value of ≈ 300 cm⁻¹ contrasts with that reported by Smith and Carter of 600 cm⁻¹.⁴⁷ This difference seems to indicate that although the bonding geometry of Pt-CO is close to that of Pt_n-CO, the existence of a metal “s band” leads to significant differences in the contribution of each distinct physical effect involved in the bonding mechanism of CO with a single Pt atom or with a Pt surface. The present value (≈ 300 cm⁻¹) is also lower than the ≈ 494 cm⁻¹ density-functional theory result reported by Ohnishi and

Watari,³² which indeed is remarkably close to the experimental EELS value for the peak assigned to the atop site (465 cm⁻¹). On the other hand, our value agrees with the peak that is experimentally assigned to the bridge CO (384 cm⁻¹). Usually, the *ab initio* cluster-model approach leads to rather accurate vibrational frequencies for the vibrational model perpendicular to the surface. In a recent work, Bagus and Illas have used an Ag₄ model to represent NO interacting above a threefold hollow site of the Ag(111) surface and found very good agreement between experimental (≈ 230 cm⁻¹) and calculated (≈ 205 cm⁻¹) values.⁴⁹ The present difference between the calculated and experimental values for this vibrational mode

TABLE I. Calculated SCF and CASSCF values for the C-Pt, $d(\text{C-Pt})$, and C-O, $d(\text{C-O})$ distances and for the vibrational mode of CO perpendicular to the surface, $\nu\text{Pt-Surf}$. Distances are in Å and frequencies in cm⁻¹. CAS1, CAS2, and CAS3 represent the different active spaces used in the CASSCF calculations. A definition of the different active spaces is given in the text.

Wave function	$d(\text{C-Pt})$	$d(\text{C-O})$	$\nu\text{Pt-Surf}$
SCF	1.989	1.100	310
CAS1	2.006	1.124	287
CAS2	1.989	1.129	295
CAS3	2.001	1.135	295
Exptl.	1.85±0.05 ^a	1.15±0.05 ^a	465 ^b

^aReference 1.

^bReferences 4 and 5.

may be due to limitations of the surface cluster model, to adsorbate-adsorbate interactions or may even indicate that the experimental assignments have to be revised (see Refs. 13 and 14). The last point may be tested by suitable cluster-model calculations for CO interacting with both atop and bridge sites and is currently being investigated in our laboratory.

Now, let us turn our attention to the main point of the present work, which concerns the internal CO vibrational mode. A summary of results for this frequency is reported in Table II where we have added the corresponding calculated and experimental values for free CO. Here, we must point out that the comparison between the calculated vibrational frequency for the stretching mode, ν_{CO} , for free and chemisorbed CO is straightforward for the SCF calculations. However, it is rather involved when CASSCF wave functions are considered. This is because even if there is a one-to-one correspondence between the active orbitals in CO and in CO-Pt₄, in the latter these active orbitals are mixed with Pt₄ orbitals and the amount of nondynamical correlation introduced by CASSCF in free and chemisorbed CO is not the same.

First of all, we will briefly comment on the results concerning the ν_{CO} for free CO. From the results on Table II we see that, compared to the experimental value, the SCF calculated ν_{CO} is too large by 275 cm⁻¹. Introduction of correlation in the π bond by considering the 1π and $2\pi^*$ molecular orbitals of CO (4 electrons in 4 orbitals in the CASSCF) reduces the difference to 149 cm⁻¹. This CAS is to be compared with CAS1 for CO-Pt₄, and to a lesser extent also to CAS2. Adding the 5σ and $6\sigma^*$ to the active space, 6 electrons in 6 orbitals, reduces the difference between the experimental and calculated value to 27 cm⁻¹. The result from this CAS is to be roughly compared with the one obtained from CAS3 of the supersystem. Finally, considering all valence molecular orbitals as active, 10 electrons in 8 orbitals, leads to a value that differs from the experimental one by 6 cm⁻¹ only. From the preceding discussion it is clear that the difference between the experimental and the SCF calculated value of the ν_{CO} is due to nondynamical correlation. This effect

TABLE II. Vibrational frequency for free and chemisorbed CO and for the vibrational shift (in cm⁻¹). CAS1, CAS2, CAS3, and CAS4 represent the different active spaces used in the CASSCF calculations. A definition of the different active spaces is given in the text.

Wave function	Free	Chemisorbed	Shift
SCF	2445	2370	-75
CAS1	2319	2251	≈ -69
CAS2	2319	2177	^a
CAS3	2197	2180	^a
CAS4	2176		
Experimental	2170 ^b	2110 ^c	-60

^aReference 13.

^bReferences 4 and 5.

^cNot displayed CASSCF of free and chemisorbed CO not comparable (see text).

should be rather similar for free and chemisorbed CO and it is expected to be larger in the latter case if the π back donation mechanism is important. Therefore, it is possible to compare SCF vibrational frequencies for free and chemisorbed CO and investigate the origin of the vibrational shift.

The SCF vibrational shift between free and chemisorbed CO is of -75 cm⁻¹ and the experimental vibrational shift is of -60 cm⁻¹. This result seems to indicate that the differential mechanisms are already contained in the SCF wave function. The absolute value of the SCF calculated ν_{CO} is too large and again, explicit consideration of nondynamical correlation effects through either CAS1, CAS2, and CAS3 largely improves the absolute value of the ν_{CO} for the chemisorbed molecule. However, for the reasons mentioned above, it is almost impossible to define an appropriate vibrational shift for the CASSCF calculations. Results from CAS1 for free and chemisorbed CO are probably comparable because the ν_{CO} is reduced from the SCF value by 126 and 119 cm⁻¹. As commented above, CAS2 and CAS3 introduce different amounts of electronic correlation in free and chemisorbed CO and it is not clear how to define an appropriate vibrational shift. However, the CASSCF values are useful because they clearly indicate the origin of the difference between the SCF calculated and the experimental values. For chemisorbed CO, both CAS2 and CAS3 calculated frequencies are in rather good agreement with experiment although comparison with respect to free CO cannot be done and the origin of the vibrational shift cannot be understood. On the other hand, the SCF values permit a direct comparison and show the existence of a vibrational shift towards the right direction.

In order to prove that the SCF vibrational shift is not fortuitous we will now investigate the different physical contributions to this shift. This analysis is possible thanks to the CSOV method, which permits a clear separation between different physical effects. The CSOV analysis starts by constructing a frozen orbital (FO) wave function from the superposition of the electronic densities of free CO and Pt₄. This FO wave function is obtained by placing CO at the equilibrium position above the Pt₄ model. However, in order to compute the vibrational frequency for the CO internal mode, we construct a series of FO wave functions using several CO distances but keeping the CO center of mass fixed at the equilibrium position. The expectation value of the energy at each CO distance computed from this FO wave function permits us to obtain a first estimate of the ν_{CO} mode in which none of the possible bonding mechanisms is allowed. At this FO step the vibrational frequency of CO is 399 cm⁻¹ larger than that of free CO also calculated at the SCF level. This large positive shift has also been found for CO on Cu_n clusters representing the Cu(100) surface^{24,25} and for CO above cluster models representing MgO(100) or NO above cluster models simulating the Cu₂O(111) surface.^{50,51} This shift has been interpreted as a "wall" effect.⁵² It is a general effect and, consequently, the same interpretation holds here for CO on Pt(111). In the next CSOV step we introduce the substrate polarization by allowing the Pt₄ orbitals to vary but using only its own vir-

tual space. To indicate this new variation we use the $V(\text{Pt}_4;\text{Pt}_4)$, symbol, where the first set in the parentheses holds for the orbitals that vary and the second set shows the orbital space in which the variation is carried out. Since only Pt_4 orbitals are varied in the Pt_4 orbital space, it is clear that the new variational degree of freedom included in $V(\text{Pt}_4;\text{Pt}_4)$ accounts for substrate polarization in response to the fixed electronic density of CO. The contribution of this physical effect to the ν_{CO} frequency is large (-90 cm^{-1}) and contributes to a decrease of the initial wall effect (see Fig. 3). Next, we allow the Pt_4 molecular orbitals to use all the virtual space and this is indicated as $V(\text{Pt}_4;\text{all})$. The $V(\text{Pt}_4;\text{all})$ variation allows donation from the occupied Pt_4 orbitals to the virtual (empty) orbitals of CO. In other words, the $V(\text{Pt}_4;\text{all})$ CSOV step allows π back donation to occur. The contribution of this effect to the vibrational shift is very large and negative (-257 cm^{-1}) and arises essentially from π back donation. This will be clearly seen when discussing the variation on the population analysis accompanying each new variational degree of freedom (Fig. 4). Polarization of CO is introduced at the $V(\text{CO};\text{CO})$ step and the contribution of this physical effect to the vibrational shift is small (-8 cm^{-1}). Finally, we allow the CO orbitals to mix with the virtual orbitals of Pt_4 ; $V(\text{CO};\text{all})$. This last effect accounts precisely for the σ donation and it is significant (-72 cm^{-1}); this is again clear from the variation of the population analysis at this CSOV step (Fig. 2). There is a small contribution (-15 cm^{-1}) due to the effects not included in the previous variations owing to the mixing between the open shell orbital, mainly of Pt_4 character, and the closed shells of CO, $V(\text{op};\text{cl})$ and to possible couplings between the different mechanisms.

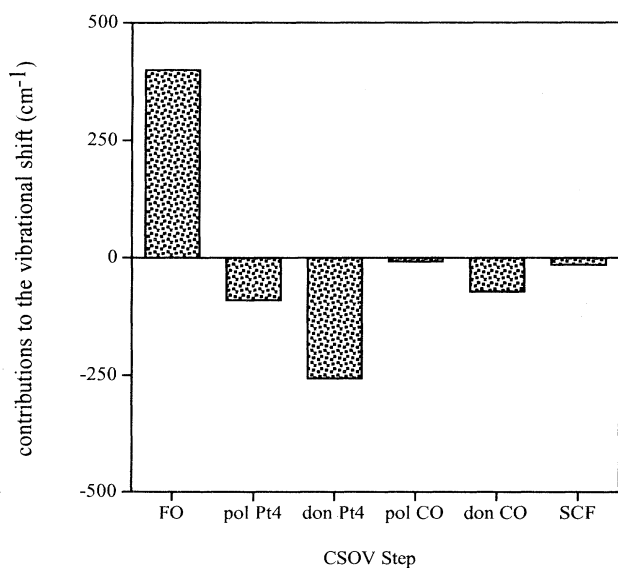


FIG. 3. Different physical contributions to the vibrational shift between free and chemisorbed CO as obtained from the CSOV decomposition. FO, pol Pt_4 , don Pt_4 , pol CO, and don CO stand for the $V(\text{Pt}_4;\text{Pt}_4)$, $V(\text{Pt}_4;\text{all})$, $V(\text{CO};\text{CO})$, and $V(\text{CO};\text{all})$ as specified in the text; SCF stands for the unconstrained Hartree-Fock calculation.

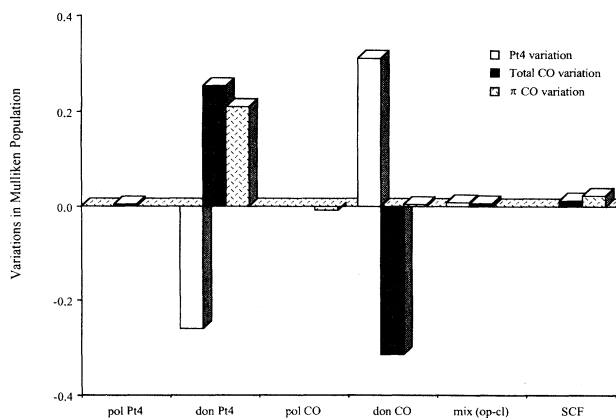


FIG. 4. Variations in the Mulliken population analysis corresponding to each step of the CSOV decomposition. The meaning of the different variations is as in Fig. 3 and mix(op-cl) stands for the $V(\text{op};\text{cl})$ variation.

The fact that this final contribution is very small is indicative that all the important mechanisms have been included in the previous variations.

To further illustrate that the mechanism responsible for the ν_{CO} vibrational frequency shift is, in fact, that suggested by Blyholder,¹⁵ we represent in Fig. 4 the variation in Mulliken population at each CSOV step. We must caution that Mulliken population analysis, although widely used, is not free of artifacts and can only provide a rough qualitative idea of the various charge transfers.⁵³ Therefore, we represent the total changes in total population for both units, Pt_4 and CO, and the variation on the π population of CO at each CSOV step. Obviously, there are significant variations at the donation steps only. From Fig. 4 it is clearly seen that at the $V(\text{Pt}_4;\text{all})$ there is a decrease in Pt_4 population that is accompanied by a similar increase on the CO electronic population. Moreover, the change on the CO population is almost exclusively of π character. This is a clear indication of the π back donation from the substrate to the adsorbate. The other significant change occurs at $V(\text{CO};\text{all})$ step and, in this case, Fig. 4 reveals that donation from CO to Pt_4 is only of σ character. Hence, Mulliken population analysis is in perfect agreement with the results obtained from frequency analysis and confirms the rightness of the Blyholder mechanism¹⁵ to interpret the vibrational shift, and the chemical bond, of CO chemisorbed on Pt(111).

To summarize the present discussion, the CSOV analyses described above show univocally that there are three important contributions to the ν_{CO} shift. One of these contributions is always positive and is due to the initial Pauli repulsion, i.e., the "wall" effect. The other two contributions are precisely the σ donation and π back donation. Both are important, although the latter is larger; its importance might be even larger if nondynamical correlation is explicitly included through either configuration-interaction or CASSCF approaches. However, the SCF and CASSCF total π population for free and chemisorbed CO is almost the same. Therefore, the increase in π population of chemisorbed with respect to

free CO cannot be attributed to nondynamical correlation effects. The CASSCF results show that the SCF analysis is correct; i.e., that the main physical effects contributing to the vibrational shift are already included in the SCF wave function. This is important because, as stated previously, comparison between the calculated free and chemisorbed CO vibrational frequencies is essential to understand the origin of the vibrational shift. This comparison can be done at the SCF level and it is difficult, if not impossible, at the CASSCF level. Here, we must point out that, at variance of CO on Cu(100) or Pd(100), the importance of the σ donation for CO on Pt(111) is large. This is because both Cu and Pd have a filled $3d\sigma$ shell and, hence, cannot add more electrons to the d shell and the only possible σ donation involves mixing of CO orbitals to the cluster virtual orbitals, which represent the metal conduction band. Clearly, the open d -shell nature of the Pt atom permits a bonding contribution through σ donation as well.

Finally, we would like to point out that the above CSOV analyses of the vibrational frequency shift and of the Mulliken populations are consistent with a CSOV analysis of the interaction energy. At the FO step the CO-Pt₄ is unbound by +2.3 eV. Substrate polarization reduces this repulsion in -1.09 eV; π back donation leads to a further reduction by -1.13 eV; CO polarization makes a small contribution of -0.12 eV but σ donation contributes by -0.81 eV. The final SCF interaction energy (-0.9 eV) differs from the sum of the previous contribution (-0.85) by 0.05 eV only. The basis set superposition error is of 0.06 eV only. These energetic contributions fully confirm the validity of the Blyholder mechanism for CO interacting with the Pt(111) surface.

IV. CONCLUSIONS

In this work we have used a cluster-model approach to describe the atop interaction of CO with a Pt(111) surface. In particular, we have analyzed the origin of the vibrational shift between free and chemisorbed CO. We have obtained SCF and CASSCF *ab initio* cluster-model wave functions, and determined the optimum geometry of chemisorbed CO and the vibrational frequencies for internal modes, which represent the normal coordinates for the motion of CO perpendicular to the surface and the CO stretching. Also, we have made use of constrained variations to analyze the origin of the vibrational

shift. The CSOV method allowed us to decompose this vibrational shift in its various physically meaningful contributions. As in the case of CO on other metal surfaces, two opposite effects have been identified. The first one is the "wall" effect originated by the Pauli repulsion between the two fixed electronic densities approaching each other. This is a large positive contribution and it is overcome by the addition of several other effects, all working in the same direction. First, there is a large contribution due to substrate polarization and next two contributions directly related to the σ donation π back donation mechanism, the latter being the largest although the former is also significant. This latter point is at variance of CO on other metal surfaces such as Cu(100) and Pd(100). This is simply because Pt has an incomplete $5d_\sigma$ shell while both Cu(100) and Pd(100) have a filled $3d_\sigma$ shell. The CSOV analysis unambiguously shows that the mechanism suggested by Blyholder does also hold for CO on Pt(111).

A last point concerns the theoretical results of Ohnishi and Watari.³² These authors have found a rather low vibrational frequency for the stretching mode of chemisorbed CO. According to our analysis the origin of this low frequency must be the donation-back donation mechanism. In our opinion, analysis of the density of states for the Pt₁₃-CO cluster presented in Ref. 32 reveals that although the $2\pi^*$ peak lies above the Fermi level it has a considerable area below the Fermi level, thus indicating the presence of π back donation.

In conclusion, the vibrational shift between the free and chemisorbed CO is originated by a large positive shift due to Pauli repulsion and two negative contributions due to σ donation and π back donation, respectively. Our theoretical analysis univocally shows that the mechanism suggested by Blyholder¹⁵ is, in fact, responsible for the observed vibrational shift.

ACKNOWLEDGMENTS

We are grateful to NATO for the Collaborative Research Grant CGR-941191. Financial support was provided by the "Comisión Interministerial de Ciencia y Tecnología" of the Spanish "Ministerio de Educación y Ciencia" under CICYT projects PB92-0766-CO2-01 and PB92-0662. The authors wish to thank the "Centre de Supercomputació de Catalunya," CESCA, for part of the calculations.

¹D. F. Ogletree, M. A. Van Hove, and G. A. Somorjai, *Surf. Sci.* **173**, 251 (1987).

²P. R. Norton, J. A. Davies, and T. E. Jackman, *Surf. Sci.* **121**, 103 (1982).

³B. Poelsema, L. K. Verheij, and H. Comsa, *Surf. Sci.* **152/153**, 496 (1985).

⁴A. M. Baró and H. Ibach, *J. Chem. Phys.* **71**, 4812 (1979).

⁵N. R. Avery, *J. Chem. Phys.* **74**, 4202 (1981).

⁶A. Crossley and D. A. King, *Surf. Sci.* **95**, 131 (1980).

⁷H. Steininger, S. Lehwald, and H. Ibach, *Surf. Sci.* **123**, 264

(1982).

⁸C. T. Campbell, G. Ertl, H. Kuipers, and J. Segner, *Surf. Sci.* **107**, 207 (1981).

⁹B. E. Hayden and A. M. Bradshaw, *Surf. Sci.* **125**, 787 (1985).

¹⁰K. P. Huber and G. Herzberg, *Molecular Spectra and Molecular Structure, Constants of Diatomic Molecules* (Van Nostrand-Reinhold, New York, 1979), Vol. 4.

¹¹H. Ibach and D. L. Mills, *Electron Energy Loss Spectroscopy and Surface Vibrations* (Academic, New York, 1982).

¹²N. Sheppard and N. T. Nguyen, *Adv. IR Raman Spectr.* **5**, 67

- (1978).
- ¹³K.-M. Schindler, Ph. Hofmann, K.-U. Weiss, R. Dippel, P. Gardner, V. Fritzsche, A. M. Bradshaw, D. P. Woodruff, M. E. Davila, M. C. Asensio, J. C. Conesa, and A. R. Gonzalez-Elipe, *J. Electron. Spectrosc. Relat. Phenom.* **64/65**, 75 (1993).
- ¹⁴M. E. Davila, M. C. Asensio, D. P. Woodruff, K.-M. Schindler, Ph. Hofmann, K.-U. Weiss, R. Dippel, P. Gardner, V. Fritzsche, A. M. Bradshaw, J. C. Conesa, and A. R. González-Elipe, *Surf. Sci.* **311**, 337 (1994).
- ¹⁵G. Blyholder, *J. Phys. Chem.* **68**, 2772 (1964).
- ¹⁶F. A. Cotton and G. Wilkinson, *Advanced Inorganic Chemistry*, 5th ed. (Wiley, New York, 1988).
- ¹⁷G. Pacchioni and J. Koutecky, *J. Phys. Chem.* **91**, 2658 (1987).
- ¹⁸M. R. A. Blomberg, C. B. Lebrilla, and P. E. M. Siegbahn, *Chem. Phys. Lett.* **150**, 522 (1988).
- ¹⁹C. M. Rohlfiing, P. J. Hay, and R. L. Martin, *J. Chem. Phys.* **85**, 1447 (1986).
- ²⁰K. Hermann, P. S. Bagus, and C. J. Nelin, *Phys. Rev. B* **35**, 9467 (1987).
- ²¹G. Pacchioni and P. S. Bagus, *J. Chem. Phys.* **93**, 1209 (1990).
- ²²J. M. Ricart, J. Rubio, F. Illas, and P. S. Bagus, *Surf. Sci.* **304**, 335 (1994).
- ²³C. W. Bauschlicher and P. S. Bagus, *J. Chem. Phys.* **81**, 5889 (1984).
- ²⁴P. S. Bagus and W. Müller, *Chem. Phys. Lett.* **115**, 540 (1985).
- ²⁵W. Müller and P. S. Bagus, *J. Vac. Sci. Technol. A* **3**, 1623 (1985).
- ²⁶P. S. Bagus and G. Pacchioni, *Surf. Sci.* **236**, 233 (1990).
- ²⁷P. S. Bagus, K. Hermann, and C. W. Bauschlicher, Jr., *J. Chem. Phys.* **80**, 4378 (1984).
- ²⁸P. S. Bagus, K. Hermann, and C. W. Bauschlicher, Jr., *J. Chem. Phys.* **81**, 1966 (1984).
- ²⁹P. S. Bagus and F. Illas, *J. Chem. Phys.* **96**, 8962 (1992).
- ³⁰J. W. Davenport, *Chem. Phys. Lett.* **77**, 45 (1981).
- ³¹S. Ishi, Y. Ohno, and B. Viswanathan, *Surf. Sci.* **161**, 349 (1985).
- ³²S. Ohnishi and N. Watari, *Phys. Rev. B* **49**, 14 619 (1994).
- ³³G. Volpilhac, M. Filali Baba, and F. Achard, *J. Chem. Phys.* **97**, 2126 (1992).
- ³⁴J. M. Ricart, A. Clotet, F. Illas, and J. Rubio, *J. Chem. Phys.* **100**, 1988 (1994).
- ³⁵P. Durand and J. C. Barthelat, *Theor. Chim. Acta* **38**, 283 (1975).
- ³⁶M. Pelissier and P. Durand, *Theor. Chim. Acta* **55**, 43 (1980).
- ³⁷J. C. Barthelat, M. Pelissier, and Ph. Durand, *Phys. Rev. A* **21**, 1773 (1981).
- ³⁸L. Fernández Pacios, *Chem. Phys. Lett.* **169**, 281 (1990).
- ³⁹S. Zurita, F. Illas, J. C. Barthelat, and J. Rubio (unpublished).
- ⁴⁰J. Rubio, S. Zurita, J. C. Barthelat, and F. Illas, *Chem. Phys. Lett.* **217**, 283 (1994).
- ⁴¹S. Zurita, J. Rubio, F. Illas, and J. C. Barthelat, *J. Chem. Phys.* (to be published).
- ⁴²T. H. Dunning, *J. Chem. Phys.* **55**, 716 (1971).
- ⁴³F. Illas, A. Márquez, S. Zurita, and J. Rubio, *J. Phys. Chem.* (to be published).
- ⁴⁴E. B. Wilson, Jr., J. C. Decius, and P. C. Cross, *Molecular Vibrations. The Theory of Infrared and Raman Spectra* (Dover, New York, 1980).
- ⁴⁵M. Dupuis, F. Johnston, and A. Márquez, IBM Corporation, Kingston, New York 12401.
- ⁴⁶A. Marquez, J. Rubio, and F. Illas, Implementation of the constrained space orbital variation method to HONDO8.5 (unpublished).
- ⁴⁷G. W. Smith and E. A. Carter, *J. Phys. Chem.* **95**, 2327 (1991).
- ⁴⁸S. Roszak and K. Balasubramanian, *J. Phys. Chem.* **97**, 11 238 (1993).
- ⁴⁹P. S. Bagus and F. Illas, *Chem. Phys. Lett.* **224**, 576 (1994).
- ⁵⁰G. Pacchioni, G. Cogliandro, and P. S. Bagus, *Int. J. Quantum Chem.* **42**, 1115 (1992).
- ⁵¹M. García-Fernández, J. C. Conesa, P. S. Bagus, J. Rubio, and F. Illas, *J. Chem. Phys.* **101**, 10 134 (1994).
- ⁵²P. S. Bagus, G. Pacchioni, and C. J. Nelin, in *Quantum Chemistry; Basic Aspects, Actual Trends*, Proceedings of the International Workshop in Quantum Chemistry, Girona, Spain, June 13–18, 1988, edited by R. Carbó, Studies in Physical and Theoretical Chemistry Vol. 62 (Elsevier, Amsterdam, 1989); J. Sauer, *Chem. Rev.* **89**, 199 (1989).
- ⁵³P. S. Bagus, F. Illas, C. Sousa, and G. Pacchioni, *Fundamental Material Science I*, edited by T. A. Kaplan, *Electronic Properties of Solids using Cluster Methods*, series editor M. F. Thorpe (Plenum, New York, 1994).